

Structural and Aerodynamics Studies on Various Wing Configurations for Morphing

D. Kumar, S. Faruque Ali, A. Arockiarajan *

* *Department of Applied Mechanics, Indian Institute of Technology Madras Chennai-600 036 (e-mail: am15d405@smail.iitm.ac.in, sfali@iitm.ac.in, aarajan@iitm.ac.in)*

Abstract: The current aircraft industry, specially unmanned aerial vehicles, is shifting from fixed wing vehicles to morphed wing. Morphing wings can create smoother aerodynamic surfaces, making an aircraft more agile and efficient than an aircraft that flies with many discrete moving surfaces. In present study, a double corrugated variable camber configuration of morphing wing with trailing edge morphing sections are proposed. The two configurations available from literature; one Fish Bone Active camber concept and other is variable camber morphing wing composed of single corrugated structure is considered for comparison of structural and aerodynamic analysis. The structural analysis of all prototype models is done using finite element analysis with actuation mechanism. Aerodynamic analysis is done using two methods; one analytical approach based on thin airfoil theory, and the other one is numerically using XFOIL, which couples a potential-flow panel method with viscous boundary-layer solver. A comparison is done on the basis of stress and deformation developed in various parts of the models. The results show that the double corrugated variable camber morphing configuration can take more structural load without harmful deformation. The aerodynamic analysis also shows that the aerodynamic efficiency of double corrugated variable camber morphing configuration is higher compared to other configurations.

© 2018, IFAC (International Federation of Automatic Control) Hosting by Elsevier Ltd. All rights reserved.

Keywords: Morphing wing, corrugated core, compliant structure.

1. INTRODUCTION

Improving performance of an aircraft is critical as it can reduce energy consumption, decrease toxic emissions and noise pollution, increase maneuverability of the aircraft. Modern aerodynamic surfaces are rigid structures with discrete sections which can move relative to each other in order to alter the aerodynamic properties of the surface. These aircrafts give high aerodynamic performance over a certain range and for a limited set of flight conditions. Outside of this range, these systems can be neutral or negatively influence the aerodynamics and hence often give lower efficiency. Researchers are focusing on morphing technology as a feasible way to enhance flight efficiency and safety of aircrafts (Thill et al. (2008); Barbarino et al. (2011)).

A morphing aircraft has the ability to change its geometry during flight. It has a lot of advantages such as improved aircraft performance by adjusting the shape corresponding to flight profiles and also reduces structural weight by removing complex mechanism of ailerons and flaps. In recent years, focus has been on to morph small aircraft (mostly unmanned aerial vehicles, or UAVs) that allow changes in one or more geometrical parameters such as span, chord length, sweep angle, dihedral angle and wing twist (Bartley-Cho et al. (2004)).

Different morphing concepts that are studied over the years have been summarized in several review papers (Chopra (2000); Barbarino et al. (2011); Weisshaar (2013)).

Much of the earlier studies have been focused on the development of active rotor systems for helicopters and tilt rotor applications. Yokozeki et al. (2006) proposed corrugated composites as candidate materials for flexible wing structures in relation to the morphing aircraft technology. Various studies on corrugated structure have been done to examine the mechanical behavior of corrugated structure. Kress and Winkler (2010) investigated the equivalent stiffness of a corrugation using unit cell analysis by curved shell theory. Dayyani et al. (2012) investigated the mechanical behavior of corrugated composite using numerical and analytical methods and compared with experimental data.

A Fish Bone Active Camber (FishBAC) concept was introduced by Woods and Friswell (2012). This model represents a biological inspired compliant structure which sustains large, continuous change in airfoil camber. Aerodynamic studies are reported which shows improvement in the lift to drag ratio of this model as compared to NACA 0012 airfoil with and without flaps.

Schmitz and Horst (2014) investigated large bending deformations and fracture mode of corrugated composites. A comparative wind tunnel testing of FishBAC morphing wing and a conventional flapped airfoil has been reported by Woods et al. (2014). The paper shows an improvement in aerodynamic efficiency in case of FishBAC morphing wing. Yokozeki et al. (2014) fabricated a variable camber morphing wing using corrugated structure with trailing edge flap section, and demonstrated the actuation of morphing wing by wind tunnel testing.

Woods et al. (2015) incorporated a coupled fluid structure interaction to calculate the deformed equilibrium configuration, aerodynamic coefficients and actuation parameters for FishBAC morphing wing. They presented that FSI analysis is capable of understanding and predicting the behavior of FishBAC morphing airfoil concept.

A variable camber morphing wing developed by Takahashi et al. (2016) which is mainly composed of corrugated structures. A morphing wing with both leading edge and trailing edge morphing has been reported. The prototype model is developed by considering finite element analysis with actuation mechanisms and with aerodynamic analysis. Wang et al. (2017) has developed analytical expression of the coupling vertical deflection under extension load for corrugated panels and verified the same with the FEM.

Corrugate structure composed of a wavy plate (see Fig. 1) was proposed by Yokozeki et al. (2006) as a candidate structure for morphing wings. When corrugated structures are applied to wing structure in such a manner such that corrugation is arranged in span direction it can withstand large load such as lift fore in span direction. While in the chord direction flexible deformation is possible because of the large anisotropic stiffness property.

In this article, a double corrugated variable camber morphing (DCVC) model is proposed for wing morphing. Using double corrugation in the model will increase the load bearing capacity of the model in span direction and also will provide the smooth bidirectional actuation of the morphing wing. The Structural and aerodynamic analysis is done for all three configurations and the comparison is done to find out the most feasible configuration.

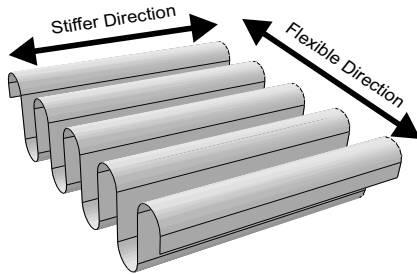


Fig. 1. An example of corrugated sheet considered in this study.

2. DOUBLE CORRUGATED VARIABLE CAMBER MORPHING WING CONCEPT

Double corrugated variable camber (DCVC) morphing wing model provides an alternative design for generating large, bidirectional changes in airfoil camber. NACA 0012 airfoil is used as the baseline for the wing model. The rigid D-spar constitutes the fixed section which is 35% (x_s) of the chord length and trailing edge morphing section is 85% (x_e) of the chord length. The structure consists of a thin chord-wise bending beam spine which coincides with the chord line of airfoil due to the symmetry.

The core of morphing section is made of double corrugated structure whose envelope coincides with the shape of airfoil (NACA 0012) and connected to a pre-tensioned Elastomeric Matrix Composite (EMC) skin surface as

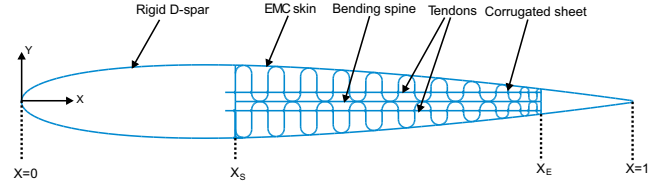


Fig. 2. Morphing wing composed of double corrugated structure with trailing edge morphing section and bending spine (This is referred to as DCVC in the text).

shown in Fig. 2. For smooth and continuous bending deflection a high stiffness, antagonistic pair of tendons are mounted. Equal and opposite displacements given to the tendons will generate a bending moment on the rigid trailing edge strip, which then induces bending of the trailing edge morphing structure to create large changes in airfoil camber.

3. STRUCTURAL ANALYSIS

Stress and deformation of the present morphing wing configuration is numerically calculated using the commercial FE software Abaqus. As the present wing configurations are uniform in the span direction, a two-dimensional numerical model is constructed. The material is assumed to behave as linear elastic. Both upper and lower skins are made up of elastomeric matrix composite. The corrugated core and bending spines are made of acrylonitrile butadiene styrene (ABS) plastic. The geometric parameters of the models are presented in table 1.

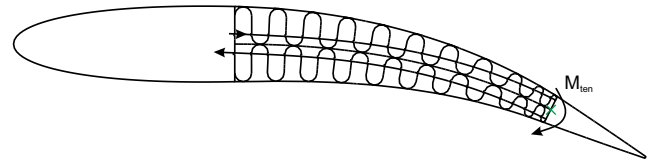


Fig. 3. Representation of tendon and trailing edge bending.

For static analysis, the structures are discretize using 2-noded cubic beam elements in a plane (B23) for DCVC model. All degrees of freedoms for the leading-edge end of the morphing section were fixed. Concentrated moments were then applied to the relevant location (Fig. 3) on the trailing-edge end as required.

Table 1: Airfoil geometry parameters

Parameter	Value
Baseline airfoil	NACA-0012
Chord (c)	300 mm
Start of morph (X_S)	105 mm
End of morph (X_E)	255 mm
Corrugated sheet thickness (t_{cs})	0.8 mm
Skin thickness (t_{sk})	1.5 mm
Tendon offset (y_{ten})	4 mm
Tendon diameter (d_{ten})	0.7 mm
Corrugated sheet modulus (E_{cs})	2.14 GPa
Spine modulus (E_{bs})	2.14 GPa
Tendon modulus (E_{ten})	131 GPa
Skin modulus (E_{sk})	4.56 MPa

3.1 Convergence study

Computational cost and time play important role in choosing the type of element for numerical analysis. A convergence study has been done for the 2D numerical static analysis. The structures are modeled using 2-noded cubic beam elements in a plane (B23). Convergence criteria is given by (1) in which δ is the tolerance value for the convergence which is selected as $1e-4$ and u_i is the nodal displacement. Fig. 4 shows the convergence study for the DCVC model, results were plotted from element size 3 mm to 0.25 mm descending order to achieve the convergence. From the simulation, it is obtained that the required size of element size for the convergence is 1 mm which takes more computational time. However, the calculated tip deflection tolerance value is less than selected value ($1e-4$).

$$\delta = \frac{u_{i+1} - u_i}{u_i} \quad (1)$$

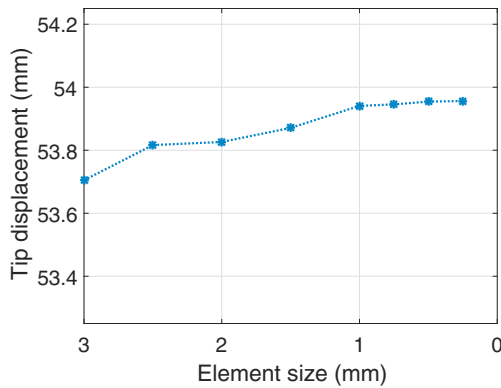


Fig. 4. Convergence study for DCVC model. Tip displacement plotted against element size.

3.2 Numerical Results

The stresses developed in corrugated structure and skin for FishBAC model by Woods and Friswell (2012), single corrugation variable camber model by Yokozeki et al. (2014) (MODEL-1) and double corrugated variable camber (DCVC) model are obtained by FE analysis are compared in Fig. 5. It can be seen in Fig. 5a and 5b that double corrugated variable camber (DCVC) model can withstand large stresses in the skin and corrugated structure as compared to other two models before reaching allowable stress (see table 2) limit of the corresponding materials.

Table 2: Allowable stress values for different materials in the structure

Component material	Allowable stress
Elastomeric matrix composite	0.29 MPa
Stringer	40 MPa

Among all three configurations, double corrugated variable camber (DCVC) model can withstand more stress in morphing skin compared to other models as shown in Fig. 5a and have approximately equal tip displacement as FishBAC model. So from the structural point of view DCVC model is a good choice for morphing wing.

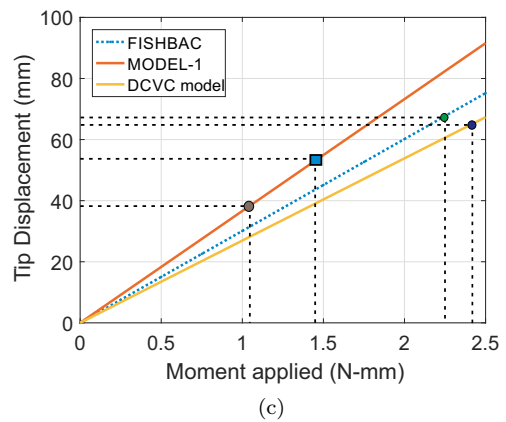
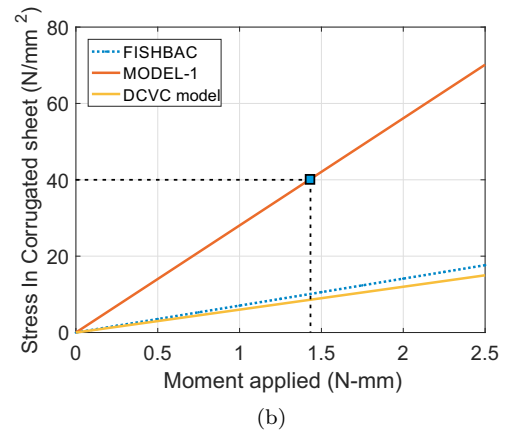
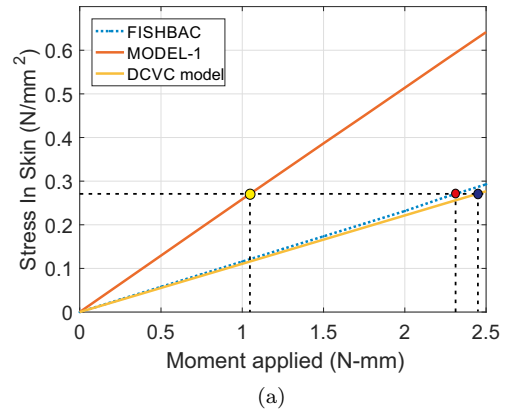


Fig. 5. Mechanical study under external moment load for various configuration. (a) Stress developed in the skin (b) Stress developed in the corrugated sheet (c) Tip displacement.

4. AERODYNAMIC ANALYSIS

4.1 Analytical method based on thin airfoil theory

In this section, a simple aerodynamic model is used for the calculation of lift coefficient based on thin airfoil theory. For incompressible, inviscid flow, an airfoil section can be modeled by a distribution of vortices along the mean camber line (See Fig. 7). This is a standard potential flow modeling technique which can give quick and reasonable estimates of lift coefficient and moment coefficient. However, as it models inviscid flow, the drag coefficient cannot

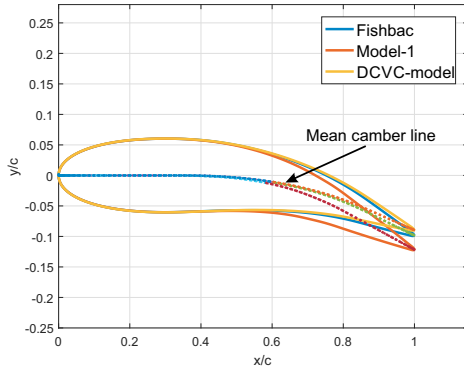


Fig. 6. Deformed structural shapes of all configurations with tendon moment ($M = 1 \text{ N-m}$).

be estimated and also it is not applicable for higher angle of attack.

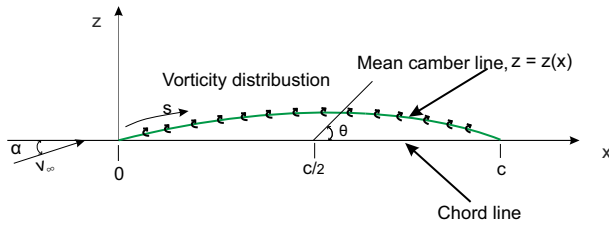


Fig. 7. Placement of the Vortex sheet on camber line.

Governing equations: The fundamental equation of thin airfoil theory is given by Eq 2, it is a statement that the camber line is a streamline of the flow.

$$\frac{1}{2\pi} \int \frac{\gamma(\theta) \sin \theta d\theta}{\cos \theta - \cos \theta_0} = V_\infty \left(\alpha - \frac{dz}{dx} \right) \quad (2)$$

The vortex distribution along the mean line forms a continuous vorticity sheet. So rather than considering the strength of point vortices, we consider the strength of the distribution per unit length, $\gamma(s)$. The distribution function is assumed to take the following form.

$$\gamma(\theta) = 2V_\infty \left(A_0 \frac{1 + \cos \theta}{dx} + \sum_{n=1}^{\infty} A_n \sin n\theta \right) \quad (3)$$

This function is Glauert's approximation and is based on Joukowski transformation results (A_0 term) which mainly covers the effect of angle of attack, plus a Fourier series variation (A_1 terms) to account for camber. It automatically obeys the Kutta condition with zero vorticity at the trailing edge. It is based on a mapped angular position (θ) rather than an exact surface location (s) to allow for ease of integration. The vorticity distribution is thus given as a function of the angular variable (θ) which is related to chord wise position x as follows,

$$x = \frac{c}{2} (1 + \cos \theta) \quad (4)$$

where (c) is the chord length. Note that chord-wise position (x) is used instead of distance along the mean line (s) for simplicity and is valid in cases where the camber height is not too large.

Substituting Eq 3 in Eq 2 and after simplification we get,

$$\frac{dz}{dx} = (\alpha - A_0) + \sum_{n=1}^{\infty} A_n \cos n\theta_0 \quad (5)$$

The solution for coefficients can now be obtained from Eq 5, given by

$$A_0 = \alpha - \frac{1}{\pi} \int_0^\pi \frac{dz}{dx} d\theta_0 A_n = \frac{2}{\pi} \int_0^\pi \frac{dz}{dx} \cos n\theta_0 d\theta_0 \quad (6)$$

Once the vorticity coefficients are found, the lift of a small element of the vortex line can be predicted from the Kutta-Joukowski law. The complete lift force is then found by summing all elements of lift from leading to trailing edge.

$$L = \rho V_\infty \sum d\Gamma = \rho V_\infty \int_0^\pi \gamma(\theta) \sin \theta d\theta \quad (7)$$

In turn, Eq 7 leads to the lift coefficient in the form

$$C_l = \frac{L}{\frac{1}{2} \rho V_\infty^2 c(1)} = \pi (2A_0 + A_1) \quad (8)$$

After substituting the value of coefficients the equation becomes

$$C_l = 2\pi \left[\alpha + \frac{1}{\pi} \int_0^\pi \frac{dz}{dx} (\cos \theta_0 - 1) d\theta_0 \right] \quad (9)$$

or

$$C_l = 2\pi [\alpha - \alpha_{L=0}] \quad (10)$$

The integral term in Eq 9 is the negative of the zero-lift angle $\alpha_{L=0}$; that is

$$\alpha_{L=0} = -\frac{1}{\pi} \int_0^\pi \frac{dz}{dx} (\cos \theta_0 - 1) d\theta_0 \quad (11)$$

4.2 Comparison of Xfoil result with thin airfoil theory result

The variation of lift coefficient with angle of attack is compared in Fig. 8 of Xfoil result with analytical result for DCVC model. The results from thin airfoil theory for DCVC model (for tendon moment $M=1 \text{ N-m}$) agrees well with Xfoil data (Inviscid and incompressible flow). Since thin airfoil theory is applicable for small angle of attack, so the variation in the plot start increasing with increase in angle of attack

4.3 Numerical method

The aerodynamic coefficients are calculated numerically using XFOIL panel method code (Drela (1989)). The code is based on potential theory with addition of viscous boundary layer solver to predict the drag and flow separation. XFOIL require the inputs as aerodynamic parameters (Angle of attack α , Reynolds number R_e and Mach number M_a) and the non-dimensionalized airfoil skin coordinates. The deformed shapes of the morphing wing configurations

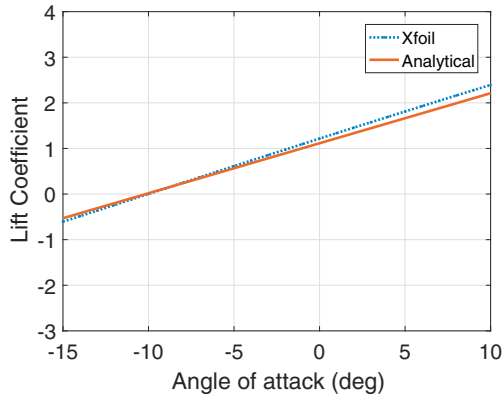


Fig. 8. Comparison of analytical lift coefficient with that of Xfoil results. The analysis is carried out assuming thin airfoil theory.

obtained by FEA without aerodynamic forces are input to the XFOIL.

The deformed shapes of all configurations obtained from FE Analysis are compared in Fig. 6 for the applied tendon moment $M=1$ N-m. As it can be seen that all wing surfaces are smoothly curved and also model-1 is going much larger deformation which will produce larger drag force.

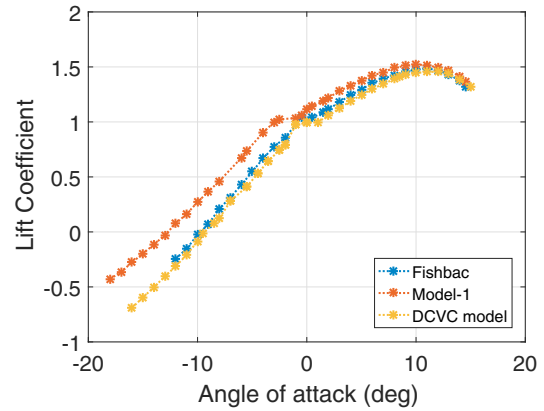
4.4 Numerical results

The lift and drag coefficients response obtained from XFOIL is shown in Fig. 9 for tendon moment $M=1$ N-m. It can be seen in Fig. 9a that lift produced by FishBAC and DCVC model are almost same. Model-1 is producing more lift but there is more drag produced (see Fig. 9b) by Model-1 as compared to other two models. Also from structural point of view Model-1 is not feasible. There is a bubble in the lift generated near angle of attack $\alpha = 0$. The immediate cause of this is not known, but it was found to be fairly repeatable. This sharp non-linearity in the performance warrants further investigation.

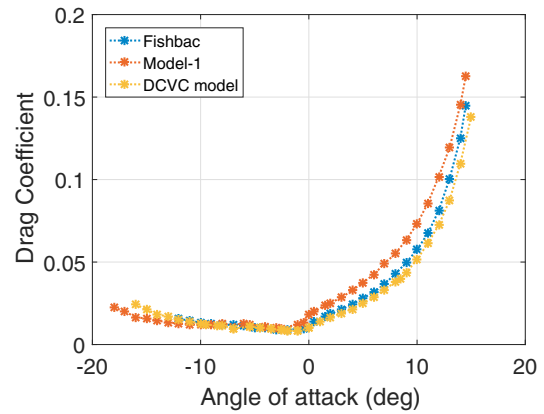
The effect of lift and drag can be combined by plotting lift-to-drag ratio (Aerodynamic efficiency) vs the angle of attack, as shown in Fig. 9c. For all configurations there is a distinct peak in the plot across the angle of attack range. Note that DCVC model is having highest peak than the other configuration. Because of larger deformation (see Fig. 6), which produced more drag force in model-1, the peak is smaller.

The effect of tendon moment on lift and drag at an angle of attack, $\alpha = 4^\circ$ is shown in Fig. 10 for all configurations. Fig. 10a shows the diminishing returns in lift is achieved with increase in tendon moment. Here also lift produced by FishBAC and DCVC model are in near equivalence. But drag produced is lesser in DCVC model as compared to FishBAC and MODEL-1.

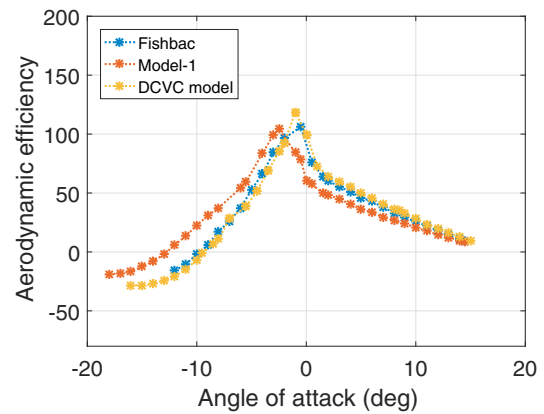
The relative aerodynamic performance of the configurations can be seen by overlaying the efficiency envelopes and comparing the performance of each configuration. This is done in Fig. 10c, here DCVC model is having higher lift to drag ratio for across applied tendon moment range, hence DCVC model has superior aerodynamic performance compared to other configurations.



(a)



(b)



(c)

Fig. 9. Variation of aerodynamic coefficients with angle of attack (With tendon moment $M = 1$ N-m) : (a) Lift coefficient (b) Drag coefficient and (c) Lift-to-Drag ratio.

5. CONCLUSION

In this study, Double corrugate variable camber (DCVC) morphing wing configuration using corrugated structure was proposed and a comparative study of three models FishBAC model, Model-1 and DCVC model on the basis of structural and aerodynamic analysis is presented. Structural analysis is done using FEM and based on this it is found that DCVC model is structurally more feasible. For aerodynamic analysis thin airfoil theory and XFOIL viscous panel-method code is used. The various results of

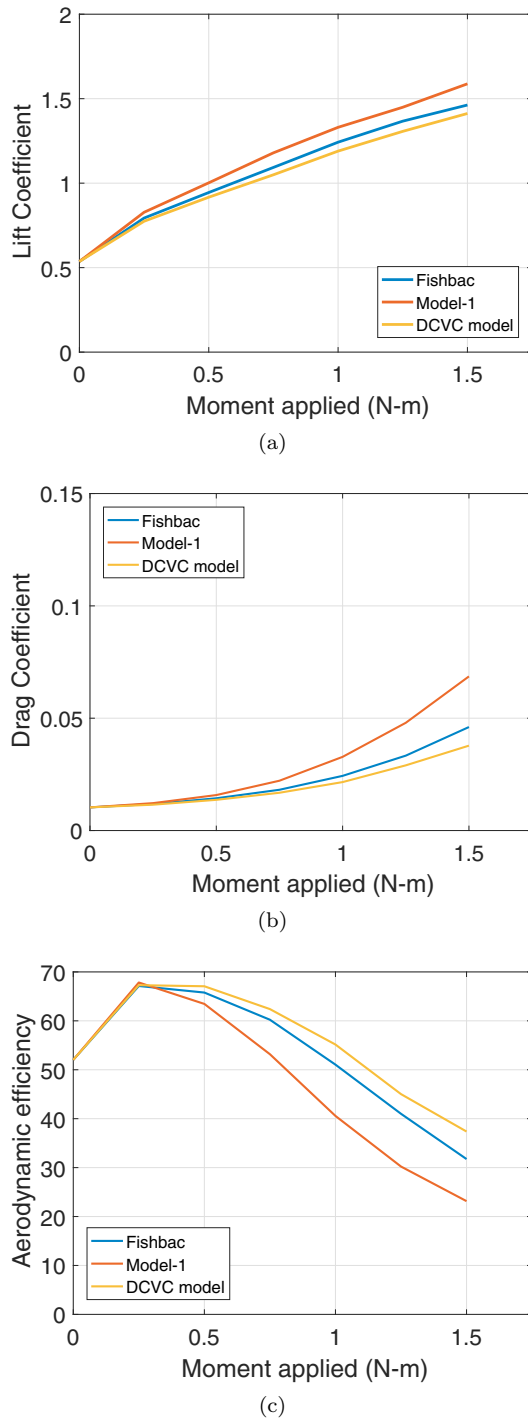


Fig. 10. Variation of aerodynamic coefficients with tendon moment : (a) Lift coefficient (b) Drag coefficient and (c) Lift-to-Drag ratio.

aerodynamic analysis show that DCVC model is having higher aerodynamic performance. So from both structural and aerodynamic point of view DCVC model is feasible and promising morphing wing concept.

ACKNOWLEDGEMENTS

The authors hereby acknowledges the funding obtained from DRDO (DRDO/DFTM/04/3304/PC/02/776/D (R&D)) through CoPT and ARDB (ARDB/01/1051810/M/I) project.

REFERENCES

- Barbarino, S., Bilgen, O., Ajaaj, R.M., Friswell, M.I., and Inman, D.J. (2011). A review of morphing aircraft. *Journal of Intelligent Material Systems and Structures*, 22, 823–877.
- Bartley-Cho, J.D., Wang, D.P., Martin, C.A., Kudva, J.N., and West, M.N. (2004). Development of high-rate, adaptive trailing edge control surface for the smart wing phase 2 wind tunnel model. *Journal of Intelligent Materials Systems and Structures*, 15, 279–291.
- Chopra, I. (2000). Status of Application of Smart Structures Technology to Rotorcraft Systems. *Journal of the American Helicopter Society*, 45, 228.
- Dayyani, I., Ziaei-Rad, S., and Salehi, H. (2012). Numerical and experimental investigations on mechanical behavior of composite corrugated core. *Applied Composite Materials*, 19, 705–721.
- Drela, M. (1989). Xfoil: An analysis and design system for low reynolds number airfoils. In *Low Reynolds number aerodynamics*, 1–12. Springer.
- Kress, G. and Winkler, M. (2010). Corrugated laminate homogenization model. *Composite Structures*, 92, 795–810.
- Schmitz, A. and Horst, P. (2014). Bending deformation limits of corrugated unidirectionally reinforced composites. *Composite Structures*, 107, 103–111.
- Takahashi, H., Yokozeki, T., and Hirano, Y. (2016). Development of variable camber wing with morphing leading and trailing sections using corrugated structures. *Journal of Intelligent Material Systems and Structures*, 1–10.
- Thill, C., Etches, J., Bond, I., Potter, K., and Weaver, P. (2008). Morphing skins. *Aeronautical Journal*, 112(1129), 117–139.
- Wang, C., Khodaparast, H.H., Friswell, M.I., and Shaw, A.D. (2017). An equivalent model of corrugated panels with axial and bending coupling. *Computers and Structures*, 183, 61–72.
- Weisshaar, T.A. (2013). Morphing aircraft systems: Historical perspectives and future challenges. *Journal of Aircraft*, 50, 337–353.
- Woods, B.K.S., Dayyani, I., and Friswell, M.I. (2015). Fluid/structure-interaction analysis of the fish-bone-active-camber morphing concept. *Journal of Aircraft*, 52, 307–319.
- Woods, B.K.S. and Friswell, M.I. (2012). Preliminary investigation of a fishbone active camber concept. *ASME Conference on Smart Materials, Adaptive Structures and Intelligent Systems*, 1–9.
- Woods, B.K., Bilgen, O., and Friswell, M.I. (2014). Wind tunnel testing of the fish bone active camber morphing concept. *Journal of Intelligent Material Systems and Structures*, 25, 772–785.
- Yokozeki, T., ichi Takeda, S., Ogasawara, T., and Ishikawa, T. (2006). Mechanical properties of corrugated composites for candidate materials of flexible wing structures. *Composites Part A: Applied Science and Manufacturing*, 37, 1578–1586.
- Yokozeki, T., Sugiura, A., and Hirano, Y. (2014). Development of variable camber morphing airfoil using corrugated structure. *Journal of Aircraft*, 51, 1–7.